Polarizabilities in the condensed phase and the local fields problem: A direct reaction field formulation

Piet Th. van Duijnen,[a] Alex H. de Vries, Marcel Swart, and Ferdinand Grozema[b]
Theoretical Chemistry, Materials Science Centre, Rijksuniversiteit Groningen, Nijenborgh 4, 9747 AG Groningen, The Netherlands

(Received 22 October 2001; accepted 13 August 2002)

A consistent derivation is given for local field factors to be used for correcting measured or calculated static (hyper)polarizabilities in the condensed phases. We show how local fields should be used in the coupled perturbative Hartree–Fock or finite field methods for calculating these properties, specifically for the direct reaction field (DRF) approach, in which a quantum chemically treated ''solute'' is embedded in a classical ''solvent'' mainly containing discrete molecules. The derivation of the local fields is based on a strictly linear response of the classical parts and they are independent of any quantum mechanical method to be used. In applications to two water dimers in two basis sets it is shown that DRF matches fully quantum mechanical results quite well. For acetone in eleven different solvents we find that if the solvent is modeled by only a dielectric continuum (hyper)polarizabilities increase with respect to their vacuum values, while with the discrete model they decrease. We show that the use of the Lorentz field factor for extracting (hyper)polarizabilities from experimental susceptibilities may lead to serious errors. © *2002 American Institute of Physics.* [DOI: 10.1063/1.1512278]

I. INTRODUCTION

Theoretical and computational studies of nonlinear optical (NLO) properties of molecules are of increasing importance for generating insight into such phenomena at the microscopic level, and may even lead to the tailoring of NLO materials. Most of these studies address only molecules or, at best, single chain oligomers or small clusters of molecules, with or without extrapolations to macroscopic systems. In contrast, most measured properties of matter stem from experiments in some condensed phase, be it in solution or in the solid state. Obviously, spectra and (hyper)polarizabilities may be, and in general are, quite sensitive to ''environmental'' effects, and to such an extent that correlating experimental and theoretical values for such properties is nontrivial.

Recently, Bishop[1] and Wortmann and Bishop[2] addressed the problem of connecting single-molecule property calculations and actual measurements. They derived local field factors from an extension of Onsager's reaction field, i.e., the simplest of the continuum models for solvating a neutral molecule, but they gave no numerical results. It seems that experimentalists and theoreticians very often rely on this ''molecule in cavity'' model in order to account for bulk effects on measured polarizabilities[3–6] where the Lorentz field[7] is taken as a local field.

Also, computational efforts to describe solvent effects on (hyper)polarizabilities are dominated by the continuum approach,[8–11] invariably reporting larger (hyper)polarizabilities in solution than in the gas phase. Recently we repeated[12] the PCM (Ref. 13) calculations of Cammi *et al.*[8] on formaldehyde in water, and found no appreciable increase in the polarizabilities if the solvent is modeled with discrete molecules. Our conclusion was that if anything happens at all, polarizabilities will be *reduced* on going from the gas to some condensed phase. More recently, Morita and Kato[14] reported similar results for simple systems in water and other liquids.

Hence, we have reasons to doubt the validity of the continuum model, in which the molecule of interest (i.e., the solute) is treated by more or less conventional quantum chemical methods, while the rest of the universe (the solvent or the rest of, e.g., a crystal) is modeled by a single parameter, i.e., the dielectric constant of the bulk material, without any reference to the structure in the condensed phase.

Here we do not want to go into all formal and practical problems associated with mixing microscopic (i.e., the wave function) and macroscopic (i.e., the dielectric constant) descriptors.[15,16] We only note that it is to be expected that the electronic properties of the solute are largely effected by the first few shells of its neighbors, and the more so the more structured these shells are. Modeling a solvent with discrete molecules gives rise to many solute–solvent interactions, which are most likely anisotropic and in principle different in each of the many different configurations needed to arrive, after averaging over the degrees of freedom, at a ''homogeneous'' solution. In contrast, the continuum solvent model starts with the assumption that the solution is homogeneous and calculates interactions between the solute and ''averaged'' molecules neglecting the instantaneous anisotropies and specific interactions. The different approaches are bound to give different results.

Figure 1 illustrates that an electronic charge distribution

[a]Author to whom correspondence should be addressed. Electronic mail: duijnen@chem.rug.nl
[b]Also at Radiation Chemistry Department, Interfaculty Reactor Institute, Delft University of Technology, Mekelweg 15, 2629 JB, Delft, The Netherlands.

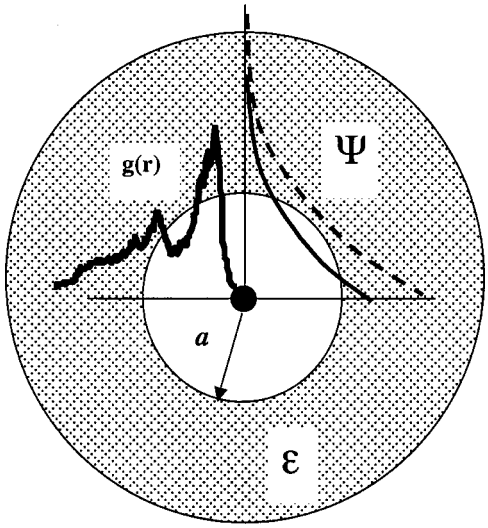

FIG. 1. An atom or molecule in a cavity of radius a in a continuum with dielectric constant ε. Vacuum (—) and "solvated" model wave functions (---) and a model radial distribution $g(r)$ for the "solvent" are shown.

in a cavity in a dielectric is always inflated, because the static dielectric will always stabilize a more extended charge distribution, leading to an increase of its polarizability.

A major problem with the continuum approach is the definition of the size and shape of the cavity. In Fig. 1 also a model radial distribution, $g(r)$, of the solvent is shown. If we want to associate the dielectric with a structureless, homogeneous continuum, it is clear that the boundary should be put at least beyond the first peak in $g(r)$. This makes the cavity so large that a neutral solute does not "feel" the solvent.[17] For smaller cavities one has to take care of the "leaking" of electron density[18–22] and of the solvent structure. The lack of solvent structure, and the fact that a static dielectric can only stabilize, makes the present continuum models unfit to account for the finer details of the solute's electronic structure.

In the direct reaction field (DRF) approach,[23,24] a quantum mechanically treated solute is surrounded by discrete solvent molecules, modeled with point charges and explicit local polarizabilities. Optionally, a dielectric continuum enveloping the complete system may be added. All charges, i.e., including the solute's electrons and nuclei, interact self-consistently with each other and with the polarizabilities. Thus, such calculations mimic at least so-called "supermolecule" SCF calculations. Hence, in this approach, all "local fields"—up to the linear response of the classical parts—are accounted for. The degrees of freedom of the discrete parts of any system can be sampled by statistical mechanics simulations, Monte Carlo (MC) or molecular dynamics (MD), at ambient temperatures. By choosing a sufficient number of configurations from the MC or MD simulations any solution structure can be accounted for. DRF has been implemented[24] in HONDO8.1,[25] GAMESS(UK),[26] and ZINDO (Ref. 27) and was applied—in its QM/MM form—to solvatochroism,[28,29] and to a reactive system,[30] while in its completely classical form[31] it is able to reproduce many body effects well in comparison with good quality SCF calculations.[32]

In this paper we will review some essential parts of the DRF method, discuss what is to be expected for polarizabilities in the condensed phase, and derive local field factors which can be used for correcting calculated or measured polarizabilities. As applications we report first fully QM and DRF results for some water dimers in order to see how DRF performs, and finally QM/MM results for acetone in eleven solvents.

II. POLARIZABILITIES OF INTERACTING MOLECULES AND THE LOCAL FIELDS

Consider a set of points (molecules or atoms) $\{\mathbf{p}\}$ with polarizabilities $\{\alpha_p\}$ in an electrostatic field $\mathbf{f}_p^0$. For the induced dipole moment $\mathbf{m}_p$ in point $\mathbf{p}$ we have[33–35]

$$\mathbf{m}_p = \alpha_p \left[\mathbf{f}_p^0 + \sum \mathbf{t}_{pq} \mathbf{m}_q \right] \tag{1}$$

with $\mathbf{t}_{pq}$ the dipole–dipole interaction tensors, given by

$$\mathbf{t}_{pq} = 3(\mathbf{r}_p - \mathbf{r}_q)(\mathbf{r}_p - \mathbf{r}_q)^{\dagger} / |\mathbf{r}_p - \mathbf{r}_q|^5 - \mathbf{I} / |\mathbf{r}_p - \mathbf{r}_q|^3, \tag{2}$$

with $\mathbf{I}$ the unit matrix. A formal solution for the $\{\mathbf{m}_p\}$ can be found by collecting the $3N^{\mathrm{pol}}$ equations into a single super matrix equation of dimension $3N^{\mathrm{pol}} \times 3N^{\mathrm{pol}}$,

$$\mathbf{M} = \tilde{\alpha}(\mathbf{F}^0 + \mathbf{T}\mathbf{M}), \tag{3}$$

where $\mathbf{F}^0$ and $\mathbf{M}$ are $3N^{\mathrm{pol}}$-dimensional vectors, and $\tilde{\alpha}$ (i.e., the diagonal blocks α_p) and $\mathbf{T}$ (i.e., the off-diagonal blocks $\mathbf{t}_{pq}$) are square $3N^{\mathrm{pol}} \times 3N^{\mathrm{pol}}$ matrices. Then

$$\mathbf{A} = [\tilde{\alpha}^{-1} - \mathbf{T}]^{-1} \tag{4}$$

is an ordinary polarizability matrix (but of an N^{pol} membered system), and

$$\mathbf{M} = \mathbf{A}\mathbf{F}^0. \tag{5}$$

The matrix $\mathbf{A}$ is obtained either by an exact matrix inversion or the associated linear equations are solved by iteration. Optionally one may reduce (parts of) $\mathbf{A}$ first to (sub) group polarizabilities,

$$\alpha_{mn}^G = \sum_{i,j}^{N^G} (A_{ij})_{mn}; \quad m,n \in \{x,y,z\} \tag{6}$$

so as to reduce the dimensionality of the problem.

For easy reference we repeat here that the induction energy is given[36] as the sum of $U_{\mathrm{stat}} = -\mathbf{M}\cdot\mathbf{F}^0$ and the polarization energy U_{pol}, i.e., the energy needed to create the induced dipoles,

$$U_{\mathrm{pol}} = \int_0^1 \mathbf{F}^0 \lambda \mathbf{M} d\lambda = \mathbf{F}^0 \mathbf{M}/2 \tag{7}$$

yielding

$$U_{\mathrm{ind}} = U_{\mathrm{stat}} + U_{\mathrm{pol}} = -\mathbf{F}^0 \mathbf{M}/2 = -\mathbf{F}^0 \mathbf{A} \mathbf{F}^0/2. \tag{8}$$

Combining with Eq. (5) we express this as a sum over the individual contributions,

$$U_{\mathrm{ind}} = -\tfrac{1}{2} \sum_i \mathbf{f}^0 \mathbf{m}_i = -\tfrac{1}{2} \sum_i \mathbf{f}_i^0 \alpha_i \mathbf{f}_i, \tag{9}$$

TABLE I. Effective polarizabilities (in Bohr^3) in clusters of *isotropic* monomers, from Eq. (4). Interatomic distance is 8 Bohr throughout.

n	Member(s)	α_{xx}	α_{yy}	α_{zz}	$\overline{\alpha}$
1					5.749
2	*a*	5.881	5.686	5.686	5.751
3	*a*	6.014	5.622	5.622	5.753
	b	5.901	5.678	5.678	5.753
5	*a*	5.827	5.827	5.601	5.752
	b[a]	5.588	5.588	5.496	5.635
7	*a*	5.762	5.762	5.762	5.762
	b[b]	5.921	5.699	5.635	5.750

[a]*xx* and *yy* values are pairwise interchanged.
[b]Values are permuted over the six members.

which is, due to the self-consistency, quadratic neither in the *permanent* fields $\mathbf{f}_i^0$ nor in the *total* (*local*) fields $\mathbf{f}_i$. Because the response of all parts is strictly linear, Eq. (8) can be written as

$$U_{\mathrm{ind}} = -\tfrac{1}{2}\sum_i \mathbf{f}_i^0 \alpha_i \mathbf{f}_i^0 (1+g_i) \tag{9a}$$

with the expression in parentheses the local field factor.

Consider two objects with polarizabilities α_1 and α_2, respectively, at a finite distance r_{12}. Then we get from Eq. (4),[35] for the components of the total polarizability of the aggregate, parallel and perpendicular to the line connecting α_1 and α_2,

$$\alpha_{\parallel} = \frac{\alpha_1+\alpha_2+4\alpha_1\alpha_2/r_{12}^3}{1-4\alpha_1\alpha_2/r_{12}^6};$$
$$\alpha_{\perp} = \frac{\alpha_1+\alpha_2-2\alpha_1\alpha_2/r_{12}^3}{1-\alpha_1\alpha_2/r_{12}^6} \quad (r_{12}^6 > 4\alpha_1\alpha_2). \tag{10}$$

Even in the case of isotropic polarizabilities, $\alpha_1=\alpha_2=\overline{\alpha}$, it follows from Eq. (10) that the total polarizability will obviously be anisotropic. If we want to define *effective* polarizabilities from Eq. (10) for the members we must (arbitrarily!) distribute the interaction term. For $\alpha_1=\alpha_2$, equipartitioning could work, leading to local anisotropy $\alpha_{\parallel}(\mathrm{local}) > \overline{\alpha}$ and $\alpha_{\perp}(\mathrm{local}) < \overline{\alpha}$, but for $\alpha \neq \alpha_2$ no scheme is obvious. One possibility is weighting the interaction term[37] with the original polarizabilities. This may work better in the general case, but it is just as arbitrary. Here the total mean polarizability $\overline{\alpha}_{12}$ will be larger than $\overline{\alpha}$. In order to find out whether this holds generally for combining arbitrary (anisotropic) polarizabilities in arbitrary relative positions we looked into a number of simple cases. We took two and three (on a line), five (on a square) and seven (on an octahedron) isotropic polarizabilities ($\overline{\alpha} \approx 6$ Bohr^3) separated by at least 8 Bohr [see Fig. 2(a)] and computed their individual and collective behavior. We took this distance because then the treatment can be completely classical.[35] For each cluster first Eq. (4) was solved and then we applied Eq. (6) to obtain the effective polarizability components for the individual members. The interaction parts in **A** were equipartitioned, i.e., each column of **A** corresponding to a particular member was contracted to a 3×3 matrix. Results are in Table I.

We see that in each cluster symmetry unique objects differ in the components of their local polarizabilities. Some are larger, some are smaller than for the monomer, depending on the symmetry and the position in the cluster. For isotropic objects on regular lattices the mean local polarizabilities are always larger than for the monomer.

Next, we constructed an anisotropic polarizability by putting the two polarizabilities of the preceding paragraphs at a distance of 2.3 Bohr following Thole's recipe,[35] contracting the whole **A** to a 3×3 matrix, and assigning the result to the center of this object. We used this as input for some simple clusters of anisotropic monomers [see Fig. 2(b)]. Results (Table II) show that now, depending on the structure of the cluster, not only the polarizability components may be smaller than that of the monomer, but also the mean polarizability. These effects scale in a simple way with the ''input'' polarizabilities as can be seen from Eq. (10).

In summary, what will happen to local polarizabilities in the condensed phases is hard to estimate without calculations. This is also demonstrated by the work of Augspurger and Dykstra[38] on acetylene clusters where for *linear* complexes an *increase* of the axial components of the linear and second hyperpolarizabilities are found, while Van Duijnen *et al.*[12] obtain for *parallel* clusters of butadienes and Kirtman *et al.*[39] for hexatrienes a *decrease* in the same properties. These authors also show that well constructed fully classical electrostatic models are able to reproduce these results.

Here we note that only a single polarizability (or susceptibility) exists for any system. The reconstruction from local contributions is in fact an abstraction, the result of which depends on the detail wanted (macroscopic with local susceptibilities, or microscopic with local polarizabilities) and—more importantly—on the partitioning of such properties. However, experimental chemists are used to such procedures: from well chosen series of compounds they derive ''bond energies'' as ''local'' contributions to heats of formation and ''ionic radii'' from crystal structures. Theoretical chemists obtain ''atomic charges'' from, e.g., a Mulliken analysis of their wave functions and we are able, following similar reasoning, to construct molecular polarizabilities from atomic ones,[35,40] although there is formally no connection between them, and—in an opposite direction—we can ''decompose'' a many center polarizability matrix **A** into local contributions, in which a one-to-one assignment of the interaction blocks to the corresponding diagonal ''local'' blocks looks like the Mulliken scheme, while a weighted assignment (e.g., with the traces of the diagonal blocks) will look like the Löwdin scheme for a population analysis. In this sense we can at least assess the local contributions to the system's polarizability, although only within an arbitrary but well defined frame work.

The extension of Eq. (5) with a dielectric continuum around the discrete part(s) is straightforward. For a discretized surface **S** [boundary element method (BEM) (Ref. 41)] the final result can be expressed in a set of linear equation of finite dimensions,[42]

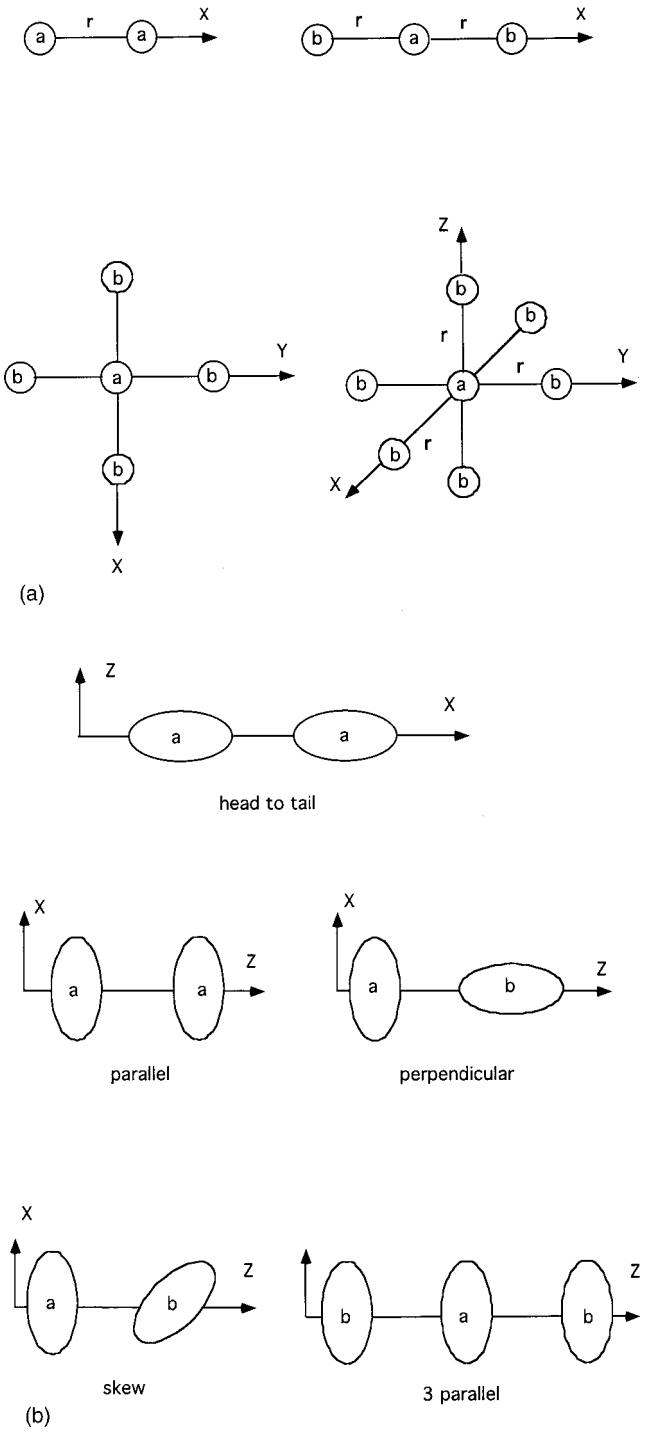

FIG. 2. (a) Arrangement of two, three, five, and seven identical isotropic polarizabilities with $r=8$ Bohr. The monomer polarizability is arbitrary taken as about 6 Bohr^3 [actually 5.88 i.e., the model value for the oxygen atom (Ref. 36) in our database]. Letters a, b, and c indicate symmetry equivalent atoms within each cluster. (b) Arrangement of two and three identical anisotropic polarizabilities. The monomer anisotropic polarizability is constructed from two monomers in (a) at 2.3 Bohr. Minimal distance between objects in the clusters is 8 Bohr.

$$\begin{bmatrix} \mathbf{M}_p \\ \mathbf{\Omega}_I \end{bmatrix} = \mathbf{A}' \begin{bmatrix} \mathbf{f}_p \\ \dfrac{\mathbf{v}_I}{2\pi(1+\varepsilon)} \end{bmatrix}, \tag{11}$$

with in the left-hand side (lhs) vector $\mathbf{M}$ representing the induced dipoles at the classical polarizable points and $\mathbf{\Omega}$ the set of induced dipoles on the surface $\mathbf{S}$. The right-hand side (rhs) matrix $\mathbf{A}'$ is given by

$$\mathbf{A}' = \begin{bmatrix} \alpha_p^{-1} + \mathbf{T}_{pq} & \nabla_p \mathbf{K}_{Ip} S_I \\ \dfrac{-\mathbf{f}_{pI}}{2\pi(1+\varepsilon)} & \mathbf{1} - \dfrac{\mathbf{K}_{IJ}}{2\pi(1+\varepsilon)} \end{bmatrix}^{-1} \tag{12}$$

with ε the (total) dielectric constant of the continuum. In the rhs vector all electrostatic source fields ($\mathbf{f}$, at the discrete polarizable points) and potentials ($\mathbf{v}$, at the representative points of $\mathbf{S}$) are collected. In Eq. (12) we have added (redundant) indices for clarity: lower case indices for discrete polarizable points and capitals for boundary elements. In the top-left block of Eq. (12b) the matrix of Eq. (4) will be recognized, while $\mathbf{K}$ and $\nabla\mathbf{K}$ are more or less complicated potential and fieldlike kernels, depending on ε and the geometry of $\mathbf{S}$.

We note that leaving out the continuum just Eq. (4) remains, while for the continuum-only approach only the bottom right block remains. But the general picture remains the same, i.e., all information about the reaction potentials are contained in a single relay matrix.

TABLE II. Effective polarizabilities (in Bohr^3) in clusters of *anisotropic* monomers. Monomer constructed from two atoms (see Table I) at a distance of 2.3 Bohr following Eq. (4). Interatomic distances between molecules ≈6 Bohr. (Numbers in *italics*: distances≈8 Bohr.)

n	Structure	Members	α_{xx}	α_{yy}	α_{zz}	$\overline{\alpha}$
1			13.904	9.248	9.248	10.800
2	head to tail	*a*	14.572	9.103	9.103	10.926
			14.261	*9.171*	*9.171*	*10.868*
	perpendicular	*a*	13.576	9.027	9.901	10.835
			13.740	*9.139*	*9.581*	*10.820*
	b	*b*	8.916	9.027	14.570	10.838
			9.084	*9.139*	*14.240*	*10.820*
	skew(45°)	*a*	13.252	8.895	10.076	10.741
			13.603	*9.087*	*9.652*	*10.781*
		b	10.919	8.894	12.418	10.744
			11.274	*9.086*	*11.983*	*10.781*
	parallel	*a*	13.121	8.895	9.909	10.642
			13.543	*9.087*	*9.570*	*10.733*
3	parallel	*a*	12.344	8.544	10.590	10.493
			13.183	*8.926*	*9.896*	*10.668*
		b	13.062	8.862	10.062	10.662
			13.506	*9.069*	*9.625*	*10.734*

III. THE ENERGY EXPRESSIONS IN THE DRF APPROACH

The DRF approach has been described many times elsewhere[23,24,43] and here we just give some relevant energy expressions. The total energy of the system can be written as

$$\Delta U^{\text{discr}} = \Delta U^{\text{QM}} + \Delta U^{\text{MM}} + \Delta U^{\text{QM/MM}}, \tag{13}$$

with ΔU^{QM} the expectation value of the vacuum Hamiltonian of the QM over the nonvacuum wave function, ΔU^{MM} the energy of the classical part(s), and $\Delta U^{\text{QM/MM}}$ the interaction in the actual configuration. Here only ΔU^{QM} and the electronic parts of $\Delta U^{\text{QM/MM}}$ are of importance. The latter is here given for the discrete case only. With $\mathbf{v}_{sp}=1/|\mathbf{r}_p-\mathbf{r}_s|$

the operator for the Coulomb potential at **p** from a source at **s**, and $\mathbf{f}_{sp}=-\nabla_p \mathbf{v}_{sp}$ the corresponding electric field operator we get

$$\Delta U_{\mathrm{el}}^{\mathrm{QM/MM}}=e\sum_{A,i,k} q_i^A\langle \mathbf{v}(k;\mathbf{i})\rangle+e\sum_{A,i,k,r,s} Z_i \mathbf{f}_{ir}A_{rs}\langle \mathbf{f}(\mathbf{s};k\rangle + e\sum_{A,i,k,r,s} q_i^A \mathbf{f}_{ir}A_{rs}\langle \mathbf{f}(\mathbf{s};k\rangle + \frac{e^2}{2}\sum_{k,l,r,s}\langle \mathbf{f}(k;\mathbf{r})\rangle A_{rs}\langle \mathbf{f}(\mathbf{s};l)\rangle, \tag{14}$$

where the $\{Z\}$ are the nuclear charges, the $\{q\}$ the classical charges, and $\langle\cdots\rangle$ denote expectation values over molecular orbitals (MOs). The A_{rs} are block matrix elements relating polarizable points at **r** and **s** of the matrix **A** (i.e., **A** or **A′**, see above), which maps the linear response functions of the classical parts. In all inductive contributions the polarization ''cost'' energy is here included, although we keep it in practice separated in order to make it also possible to deal with nonequilibrium situations. For clarity we have made explicit the electronic charge (e) and the electron (or, rather MO) labels (k,l) in the potential and field expectation values.

IV. SYSTEM IN AN EXTERNAL FIELD

If a system is placed in an external electrostatic field, **f**, the change in energy can be expanded as

$$\Delta U(\mathbf{f})=-\left(\mu_i^0\mathbf{f}_i+\frac{1}{2!}\alpha_{ij}\mathbf{f}_i\mathbf{f}_j+\frac{1}{3!}\beta_{ijk}\mathbf{f}_i\mathbf{f}_j\mathbf{f}_k+\frac{1}{4!}\gamma_{ijkl}\mathbf{f}_i\mathbf{f}_j\mathbf{f}_k\mathbf{f}_l+\cdots\right);\quad \{i,j,k\}\in\{x,y,z\}, \tag{15}$$

with μ^0 the permanent dipole moment, α the polarizability tensor, and β and γ the first and second hyperpolarizabilities of the system. The indices are summed over (all permutations of) the Cartesian axes x, y, and z.

One can use Eq. (15) by applying various field strengths and determine numerically the derivatives of $\Delta U(\mathbf{f})$ to obtain the dipole moment and the (hyper)polarizabilities. This finite field (FF) approach is applicable to any type of wave function for QM. For closed shell, single determinant wave functions, the coupled perturbative Hartree–Fock (CPHF) (Ref. 44) method is a good alternative which is generally faster. The first and second derivatives of the total energy of QM (in the Born–Oppenheimer approximation) in vacuum w.r.t. the components of the field **f** are

$$\frac{\partial[\Delta U(\mathbf{f})]}{\partial f_i}=-\langle\mu_i^{\mathrm{tot}}\rangle;\quad \frac{\partial^2[\Delta U(\mathbf{f})]}{\partial f_i\partial f_j}=-e\frac{\partial\langle\mu_i^{\mathrm{el}}\rangle}{\partial_j}\equiv\alpha_{ij}, \tag{16}$$

with μ^{tot} the total dipole moment and μ^{el} the electronic contribution. In CPHF, applied to a molecule in vacuum, one takes the electronic part of the first derivative of $\Delta U(\mathbf{f})$ as the perturbing Hamiltonian,

$$h_{mn}^i\equiv -e(\mu_{mn}^0)^i \tag{17}$$

with μ the dipole operator, e the elementary charge, while m,n refer to basis functions. For the first and second field derivatives of the wave function we write[25]

$$\frac{\partial\Psi}{\partial f_i}\equiv|\Psi^i\rangle;\quad \frac{\partial^2\Psi}{\partial f_i\partial f_j}\equiv|\Psi^{ij}\rangle, \tag{18a}$$

then we can construct the following density matrices,

$$\mathbf{D}^0=|\Psi^0\rangle\langle\Psi^0|;\quad \mathbf{D}^j=|\Psi^j\rangle\langle\Psi^0|,\qquad \mathbf{D}^{jk}=|\Psi^j\rangle\langle\Psi^k|;\quad \mathbf{D}^{jkl}=|\Psi^j\rangle\langle\Psi^{kl}|, \tag{18b}$$

where it is assumed that contributions obtained by permuting the indices are summed. Then we have to fourth order,

$$\mu_i^{\mathrm{el}}=\mathrm{Tr}(\mathbf{D}^0\mathbf{h}^i);\quad \alpha_{ij}=\mathrm{Tr}(\mathbf{D}^j\mathbf{h}^i),\qquad \beta_{ijk}=\mathrm{Tr}(\mathbf{D}^{jk}\mathbf{h}^i);\quad \gamma_{ijkl}=\mathrm{Tr}(\mathbf{D}^{jkl}\mathbf{h}^i). \tag{19}$$

Both approaches, FF and CPHF are easily extended to the DRF method. If we write for the solute's contribution to the change in total energy,

$$(\Delta U_{\mathrm{DRF}}^{\mathrm{solute}}(\mathbf{f}))_i=-[\mu_{\mathrm{DRF}}^{\mathrm{solute}}+\mu^{\mathrm{QM/MM}}]_i\ f_i+\cdots=-[\mu_{\mathrm{DRF}}^{\mathrm{solute}}+\mu^{\mathrm{QM/MM}}]_i\ f_i^{\mathrm{ext}}(1+g_i)+\cdots \tag{20}$$

with **f** the local field at QM and $\mu^{\mathrm{QM/MM}}$ stands for all dipoles induced by the solute in the classical parts, it will be clear that the perturbing operator for CPHF must be adapted to reflect the use of the actual field at QM. For FF it is only needed to add the external field to the sources in Eq. (12a) and solve the resulting linear equations.

From Eq. (8) we obtain for the solute's contribution to the total induction energy,

$$\begin{aligned}(U_{\mathrm{ind}}^{\mathrm{solute}})_{ij}&=-\tfrac{1}{2}\ f_i^{\mathrm{ext}}\{\alpha_{ij}^{\mathrm{eff}}\}f_j\\&=-\tfrac{1}{2}\ f_i^{\mathrm{ext}}\{\alpha_{ij}+\tfrac{1}{3}[\beta_{ijk}+\tfrac{1}{4}\gamma_{ijkl}f_l]f_k\}f_j\\&=-\tfrac{1}{2}\ f_i^{\mathrm{ext}}\{\alpha_{ij}+\tfrac{1}{3}[\beta_{ijk}+\tfrac{1}{4}\gamma_{ijkl}f_l^{\mathrm{ext}}(1+g_l)]\\&\quad\times f_k^{\mathrm{ext}}(1+g_k)\}f_j^{\mathrm{ext}}(1+g_j)\end{aligned} \tag{21}$$

and U_{ind} should be expanded in the various $f^{\mathrm{ext}}(1+g)$ rather than in f^{ext} itself when using the FF method.

Since we require the usual symmetry for the (hyper)polarizabilities,

$$\alpha_{ij}=\alpha_{ji};\quad \beta_{ijk}=\beta_{kij}=\beta_{jki}=\cdots;\qquad \gamma_{ijkl}=\gamma_{lijk}=\gamma_{klij}=\gamma_{jkli}=\cdots, \tag{22}$$

the local field factors are obtained from the following expressions:

$$\frac{\partial^2 U_{\mathrm{ind}}^{\mathrm{solute}}}{\partial f_i\partial f_j}=-\frac{1}{2}[\alpha_{ij}(1+g_j)+\alpha_{ji}(1+g_i)]=-\frac{\alpha_{ij}}{2}[(1+g_j)+(1+g_i)], \tag{23a}$$

$$\frac{\partial^3 U_{\rm ind}^{\rm solute}}{\partial f_i \partial f_j \partial f_k} = -\frac{1}{3}[\beta_{ijk}(1+g_j)(1+g_k)+\beta_{kij}(1+g_i)(1+g_j) + \beta_{jki}(1+g_i)(1+g_k)+\cdots] = -\frac{\beta_{ijk}}{3}[(1+g_j)(1+g_k) + (1+g_i)(1+g_k)+(1+g_i)(1+g_j)], \quad (23b)$$

$$\frac{\partial^4 U_{\rm ind}^{\rm solute}}{\partial f_i \partial f_j \partial f_k \partial f_k} = -\frac{1}{4}[\gamma_{ijkl}(1+g_l)(1+g_k)(1+g_j) + \gamma_{lijk}(1+g_k)(1+g_j)(1+g_i)+\cdots] = -\frac{\gamma_{ijkl}}{4}[(1+g_j)(1+g_k)(1+g_l) + (1+g_i)(1+g_k)(1+g_l)+(1+g_i)(1+g_j) \times(1+g_l)+(1+g_i)(1+g_j)(1+g_k)]. \quad (23c)$$

The $\{g\}$ in Eqs. (23) depend on the actual partitioning of the system, on its geometry and the particular point(s) for which the fields are to be evaluated. Obviously one can calculate g's for any point, but only the assumed center of the electric moments and polarizabilities of QM is needed, for which usually the center of mass is chosen. We note that the dipole moment for a neutral molecule and all polarizabilities are origin independent. For example, take two different centers, **R** and **X**, for evaluating the dipole integrals. Then, e.g., for the linear polarizability one has

$$\alpha_{ij}(\mathbf{R}) = {\rm Tr}(\mathbf{D}^j\mathbf{h}^i(\mathbf{R})) = \sum_{m,n} D^j_{mn} h^i_{nm}(\mathbf{R}),$$

$$\alpha_{ij}(\mathbf{R}') = {\rm Tr}(\mathbf{D}^j\mathbf{h}^i(\mathbf{R}')) = \sum_{m,n} D^j_{mn}[h^i_{nm}(\mathbf{R}) - (R_i - X_i)S_{nm}] = {\rm Tr}(\mathbf{D}^j\mathbf{h}^i(\mathbf{R})) - (R_i - X_i){\rm Tr}(\mathbf{D}^j\mathbf{S}) = {\rm Tr}(\mathbf{D}^j\mathbf{h}^i(\mathbf{R})), \quad (24)$$

with S the overlap matrix. ${\rm Tr}(\mathbf{D}^j\mathbf{S})$ is the (field) derivative of the number of electrons, which is obviously zero.

The actual g's to be calculated also depend on the constituents of the complete system. For a DRF cluster in vacuum $\mathbf{f}^{\rm ext}$ resides in the vacuum and the solute's electrons feel this field modulated by the fields from the induced dipoles at the classical polarizabilities, while the dipoles induced by QM only feel $\mathbf{f}^{\rm ext}$. Hence we have for the perturbing operator,

$$(h_{mn})^i_{\rm DRF} = -e\{(\mu^i_{mn}(1+g_i^{\rm discrete}) + [\mu^{\rm QM/MM}_{\rm discrete}]_{mn})\}, \quad (25)$$

where the $[\mu^{\rm QM/MM}_{\rm discrete}]_{mn}$ are the integrals defining the dipoles induced by QM at the discrete polarizabilities. If a continuum is present we assume that $\mathbf{f}^{\rm ext}$ resides in that continuum, leading to

$$(h_{mn})^i_{\rm DRF} = -e\{(\mu^i_{mn}(1+g_i^{\rm discrete}) + [\mu^{\rm QM/MM}_{\rm discrete}]_{mn}) \times(1+g_i^{\rm boundary}) + [\mu^{\rm QM/MM}_{\rm boundary}]_{mn}\} \quad (26)$$

since all charge distributions inside the cavity feel the field from the continuum polarization, while the dipoles induced on the boundary, represented by the $[\mu^{\rm QM/MM}_{\rm boundary}]_{mn}$ integrals, feel only $\mathbf{f}^{\rm ext}$. All necessary ingredients for calculating the g's referring to any point are available after solving the appropriate linear equations with appropriate source fields.

The $g_i^{\rm boundary}$ depend on the shape of cavity. For a spherical cavity the field $\mathbf{f}^{\rm cav}$ due to the polarization of the continuum, *inside* this cavity is uniform and parallel to $\mathbf{f}^{\rm ext}$, and is given by[7]

$$\mathbf{f}^{\rm cav} = [3\varepsilon/(2\varepsilon+1)]\mathbf{f}^{\rm ext} = (1+g^{\rm cav})\mathbf{f}^{\rm ext}; \quad g^{\rm cav} = (\varepsilon-1)/(2\varepsilon+1). \quad (27)$$

We note that for a sizable, practically spherical, discrete cluster the QM part does not generate appreciable induced dipoles on the boundary, so we can use $\mathbf{f}^{\rm cav}$ directly without the continuum being actually present, in which case Eq. (30) is reduced to

$$(h_{mn})^i_{\rm DRF} = -e\{(\mu^i_{mn}(1+g_i^{\rm discrete}) + [\mu^{\rm QM/MM}_{\rm discrete}]_{mn}) \times(1+g_i^{\rm cav})\} \quad (28)$$

which will enable one to apply this as a ''bulk correction'' to any cluster of roughly spherical shape.

The Lorentz field[7] is often used for correcting measured susceptibilities with

$$\mathbf{f}^{\rm lorentz} = \frac{\varepsilon+2}{3}; \quad g^{\rm lorentz} = \frac{\varepsilon-1}{3} \quad (29)$$

for all directions and disregarding all actual local polarizations. In the derivation of Eq. (29) it is assumed that the (macroscopic!) system is uniformly polarized, and hence, formally, the Lorentz field is only applicable for pure substances. However it is a rather crude approximation and may lead to substantial errors,[2] in particular in the microscopic description we have in mind. We have

$$(h_{mn})^i_{\rm DRF} = -e\{\mu^i_{mn}(1+g^{\rm lorentz})\}. \quad (30)$$

From the CPHF calculations one obtains, using the perturbation from Eq. (25), (26), or (27), a linear polarizability $\alpha^{\rm CPHF}$ which contains the polarizations of the classical parts. From the associated density matrices the solute's electronic contributions is calculated and corrected by applying the appropriate field factors of Eq. (23a),

$$\alpha^{\rm raw}_{ij} = \frac{2\,{\rm Tr}(\mathbf{D}^j\mathbf{h}^i_0)}{[(1+g_j)+(1+g_i)]}, \quad (31)$$

where the zero in Eq. (31) emphasizes that only the vacuum dipole integrals of QM are used. On the resulting $\alpha^{\rm raw}$ the total field on QM is first applied to obtain the dipole induced by this field which is present in the self consistent solution of the CPHF/DRF procedure because of the presence of terms like $[\mu^{\rm QM/MM}_{\rm discrete}]_{mn}$ in the perturbing operator. Then the corresponding reaction field is obtained by solving Eq. (12) with this induced dipole as only source. This reaction field, yielding $g^{\rm ind}$, is added to the total field at QM and then $\alpha^{\rm raw}$ is corrected again with this final field,

TABLE III. Comparison of full quantum and (exact) DRF calculations for two water dimers using two basis sets. The first molecule is in the $Z=0$ plane with its dipole moment along the *Y*-axis. Left-hand columns: Sadlej basis (Ref. 46); right-hand columns DZP basis (Ref. 47). Point charges on the classical molecules reproduce the monomer vacuum dipole moment. For the classical molecular polarizability the calculated vacuum monomer tensor was used. All data in atomic units. (top) Parallel dimer constructed by shifting an image of the monomer by 5 Bohr in the *Z*-direction. (bottom) Hydrogen bonded water dimer constructed by shifting an image of the monomer by 5.325 Bohr in the OH direction. Parameter as above.

Property	mono	drf(1)	drf(2)	dimer	BSSE	dimer-BSSE	drf (1+2)	mono	drf(1)	drf(2)	dimer	BSSE	dimer-BSSE	drf (1+2)
μ_y	−0.79	−0.74	−0.74	−1.48	0.0	−1.48	−1.48	−0.89	−0.85	−0.85	−1.69	0.0	−1.69	−1.70
α_{xx}	9.40	8.83	8.83	17.95	−0.01	17.96	17.66	7.43	7.20	7.20	14.70	0.16	14.54	14.40
α_{yy}	8.66	8.13	8.13	16.50	−0.02	16.52	16.26	5.59	5.44	5.44	11.01	0.11	10.90	10.89
α_{zz}	7.90	8.68	8.68	16.22	0.08	16.14	17.36	3.03	3.16	3.16	7.37	2.22	5.15	6.31
$\overline{\alpha}$	8.65			16.89		16.87	17.09	5.35	5.27	5.27	11.02		10.20	10.54
β_{xxy}	10.5	11.1	11.1	21.3	0.3	21.0	22.2	20.8	20.1	20.1	39.0	0.22	38.8	40.1
β_{yyy}	5.1	8.4	8.4	16.6	2.0	14.6	16.8	10.0	9.9	9.9	18.5	−0.27	18.7	19.8
β_{yzz}	−0.6	1.5	1.5	5.1	1.3	3.8	3.0	0.6	0.8	0.8	3.5	0.7	2.8	1.6
β_y	9.0	12.6	12.6	25.8		23.6	25.2	18.9	18.4	18.4	36.6		36.2	36.9
$\boldsymbol{\beta}\cdot\boldsymbol{\mu}$	−7.1			−38.2		−35.0	−37.3	−16.7	−15.7	−15.7	−61.7		−61.3	−62.9
γ_{xxxx}	501	470	470	974	62	912	940	192	179	179	320	3	317	357
γ_{xxyy}	292	273	273	553	23	530	546	140	132	132	238	2	236	264
γ_{xxzz}	296	280	280	626	41	585	560	11	12	12	69	111	−42	24
γ_{yyyy}	790	736	736	1551	124	1427	1472	61	58	58	99	0	99	117
γ_{yyzz}	331	311	311	702	60	641	621	6	7	7	29	61	−32	14
γ_{zzzz}	1223	1501	1501	3246	299	2947	3002	12	14	14	728	1399	−671	28
$\overline{\gamma}$	871			1906		1759	1773	116	110	110	364		14	221
μ_x	0.00	−0.05	0.00	0.13	0.00	0.13	−0.05	0.00	0.00	0.06	0.12	0.00	0.12	0.06
μ_y	−0.79	−0.82	−0.79	−1.62	0.00	−1.62	−1.60	−0.89	−0.89	−0.90	−1.82	0.00	−1.82	−1.79
α_{xx}	9.41	9.68	9.40	19.29	−0.01	19.30	19.08	7.43	7.44	7.71	15.39	0.21	15.18	15.15
α_{yy}	8.66	8.66	8.66	17.45	0.01	17.44	17.32	5.59	5.59	5.67	11.60	0.31	11.29	11.26
α_{zz}	7.90	7.48	7.90	15.16	0.05	15.11	15.38	3.03	3.03	3.00	5.98	0.05	5.94	6.03
$\overline{\alpha}$	8.66	8.61	8.65	17.30		17.28	17.26	5.35	5.35	5.46	10.99		10.80	10.81
β_{xxx}	0.0	−0.6	0.0	2.8	0.0	2.8	−0.6	0.0	0.0	−1.0	1.1	1.1	0.0	−1.0
β_{xxy}	10.5	8.1	10.5	19.1	−0.2	19.3	18.6	20.8	20.8	22.5	37.7	−2.0	39.6	43.4
β_{xyy}	0.0	0.0	0.0	0.0	0.0	0.0	0.0	0.0	0.0	0.0	0.0	0.0	0.0	0.0
β_{xzz}	0.0	−1.6	0.0	0.7	0.0	0.7	−1.6	0.0	0.0	−0.7	2.2	1.7	0.5	−0.7
β_{yyy}	5.1	5.7	5.1	11.1	1.4	9.7	10.8	10.0	10.0	10.2	18.9	1.4	17.5	20.2
β_{yzz}	0.0	0.0	0.0	0.0	0.0	0.0	0.0	0.0	0.0	0.0	0.0	0.0	0.0	0.0
β_x	0.0	−1.1	0.0	3.0		3.1	−1.1	0.0	0.0	−0.8	1.9		0.4	−0.8
β_y	9.0	8.6	9.0	17.5		16.5	17.6	18.8	18.9	19.9	34.6		34.8	38.8
$\boldsymbol{\beta}\cdot\boldsymbol{\mu}$	−7.1	−6.9	−7.1	−27.9		−26.3	−28.1	−16.7	−16.8	−18.0	−62.7		−63.4	−69.5
γ_{xxxx}	502	508	501	1069	40	1029	1009	192	193	230	552	116	436	423
γ_{xxyy}	293	306	292	636	1	635	598	140	140	159	437	114	323	300
γ_{xxzz}	296	262	296	548	32	516	559	11	11	11	20	7	13	22
γ_{yyyy}	791	730	790	1614	76	1539	1520	61	61	65	311	216	96	126
γ_{yyzz}	331	284	331	603	24	579	615	6	6	6	13	7	6	12
γ_{zzzz}	1224	1037	1223	2256	177	2079	2261	12	12	12	23	2	22	24
$\overline{\gamma}$	872	796	871	1703		1621	1667	116	116	132	365		247	248

$$\alpha_{ij}^{\mathrm{corr}}=\frac{2\ \mathrm{Tr}(\mathbf{D}^j\mathbf{h}_0^i)}{[(1+g_j+g_j^{\mathrm{ind}})+(1+g_i+g_i^{\mathrm{ind}})]}. \tag{32}$$

The final field is also used for the local field corrections in Eqs. (23b) and (23c).

The ε in Eqs. (27) and (28) is the optical rather than the total dielectric constant since experiments for measuring polarizabilities are usually of an optical nature. The same holds indirectly for Eq. (26), where the $[\mu_{\mathrm{boundary}}^{\mathrm{QM/MM}}]_{mn}$ are also related to the optical dielectric constant, although the unperturbed wave function in this case is of course "solvated" by a continuum having the full dielectric constant.

Finally we note that the original reaction field (i.e., without external field) and the fields due to the classical point charges have no direct influence on the polarizability but they have an effect on the wave function, of course.

V. APPLICATIONS

A. Water dimers, comparing DRF with full quantum calculations

Already in Ref. 12 we have shown that DRF, in its QM/MM form, reproduces the results of fully quantum chemical calculations of the water dimer in various geometries fairly well. At that time we did not treat the local fields explicitly. For easy reference we give here the results of calculations on similar systems which can be compared with fully QM calculations. We took two water dimers, one in a parallel, the other in a hydrogen bonded geometry. They were treated in a standard SCF/CPHF procedure, and corrected for the basis set superposition error [BSSE (Ref. 45)]. Next we treated the various monomers with the CPHF/DRF procedure as described above with the "other" monomers

TABLE IV. Some properties of the solvents. *M*: molecular weight; *d*: density; ε: dielectric constants; *r*: effective molecular radius (from the density); *nD*: refractive index: $\overline{\alpha}$ (LL): experimental molecular polarizability (Lorentz–Lorenz from *nD*); $\overline{\alpha}$ (model): molecular polarizability from Ref. 40 and the actual geometry. μ: calculated vacuum dipole moment: *N*: number of molecules in the cluster simulations.

Solvents		*M*	*d*	ε	$\varepsilon(\infty)$	*r*	*nD*	$\overline{\alpha}$ (LL)	$\overline{\alpha}$ (model)	μ	*N*
water	H_2O	18.00	0.9982	78.5	1.77654	3.640	1.3329	9.92	10.06	2.23	50
acetonitrile	CH_3CN	41.05	0.7857	37.5	1.80695	5.189	1.3442	29.63	34.28	4.19	40
methanol	CH_3OH	32.04	0.7914	32.0	1.76571	4.766	1.3288	22.02	26.45	2.22	40
ethanol	C_2H_5OH	46.07	0.7893	24.3	1.85259	5.384	1.3611	34.56	35.25	1.81	40
acetone	C_2H_6CO(l)	58.08	0.7899	20.7	1.84634	5.815	1.3588	43.28	42.81	3.34	40
	C_2H_6CO(g)	58.08	0.0026		1.00220	39.141	1.0011	43.99			
1,2-dichloroethane	$C_2H_4Cl_2$	98.96	1.2351	10.7	2.08745	5.984	1.4448	57.03	56.04	0.00	40
chloroform	$CHCl_3$	119.4	1.4830	4.8	2.09063	5.993	1.4459	57.42	57.51	1.14	50
benzene	C_6H_6	78.12	0.8787	2.3	2.25330	6.195	1.5011	70.09	70.12	0.00	40
dioxane	$C_4H_8O_2$	88.12	1.0337	2.2	2.02322	6.109	1.4224	58.00	68.11	0.00	40
tetra	CCl_4	153.82	1.5940	2.2	2.09063	6.366	1.4459	68.83	68.46	0.00	50
cyclohexane	C_6H_{12}	84.16	0.7785	2.0	2.03524	6.612	1.4266	74.20	72.44	0.00	40

acting as classical partners. In order to compare the results with the fully QM results the individual DRF results should be added, of course. We used two basis sets: a Sadlej basis[46] and a standard DZP (Ref. 47) basis.

Usually we expand the inducing and response potentials and fields around the solute's atomic centers[24] but for larger basis sets this expansion fails. Therefore we reanimated an ''exact'' version of HONDO/DRF.[48] This version is much more demanding on CPU time and storage, e.g., one has to generate, store, and manipulate at least three one-electron matrices for each classical polarizable point for the reaction fields, which turns the use of very large basis sets impractical. Table III summarizes the results obtained with this program. In this table the most important columns to compare are headed ''dimer-BSSE'' and ''drf1+drf2.'' Components which are zero by symmetry are omitted.

First we note that the Sadlej basis gives for the monomer about 85% of the experimental mean linear polarizability ($\overline{\alpha}$) for water (see Table IV). It has about the correct (or rather lack of) anisotropy. In contrast, the DZP basis produces a much too large anisotropy and about 50% of the experimental $\overline{\alpha}$. However this is not the issue here: we want to demonstrate how DRF performs. The left-hand columns of Tables III (for the Sadlej basis) show—regarding the simplicity of our model—excellent agreement between fully quantum and DRF calculations. It is important to note that the BSSEs in α and β are modest, but they are in γ more significant. For the DZP basis the BSSEs in α and β are still acceptable but those in the γ_{xxzz} and γ_{zzzz} components for the parallel geometry are much too large, showing that this basis set is inadequate to arrive at better than qualitative results for this property. In the hydrogen bonded complex the errors are less dramatic and in particular the averaged intrinsic properties obtained in the different basis sets is satisfactory. In general we may conclude that our half classical DRF method is able to mimic fully quantum mechanical calculations apparently for any basis set, and that even for sensitive higher order properties discussed here. Hence we trust that DRF can be applied for systems the size of which forbids a fully quantum mechanical treatment.

TABLE V. Results for a single solute/solvent configuration of acetone in acetone (a.u.).

Property		$\overline{\alpha}^{\text{CPHF a}}$	$\overline{\alpha}^{\text{raw b}}$	$\overline{\alpha}^{\text{corrected c}}$	$\overline{\gamma}^{\text{corrected}}$	$\boldsymbol{\beta}\cdot\boldsymbol{\mu}^{\text{corrected}}$	Field factors[d]		
	option						*x*	*y*	*z*
basis					Sadlej				
vac				38.59	4806	−60.4			
drf(discr.)	nobulk	24.29	30.21	35.99	4211	−6.2	0.83	0.84	0.85
basis					dzp				
vac				33.35	809	−56.6			
drf(bem)		63.46	46.21	37.05	998	−63.0	1.23	1.22	1.15
drf(discr.)	nobulk	21.87	26.42	31.29	390	−52.9	0.83	0.84	0.85
	bulk	28.62	29.82	30.37	476	−40.0	0.97	0.99	0.99
basis					dzv				
vac				31.99	898	−68.37			
drf(bem)	bem	60.28	44.31	36.88	1120	−76.2	1.23	1.22	1.15
drf(discr.)	nobulk	19.94	24.62	29.31	646	−59.0	0.83	0.84	0.85
	bulk	27.71	28.93	29.06	538	−50.6	0.97	0.99	0.99
	Lorentz	48.65	39.63	31.48	837	−84.80	1.26	1.26	1.26
	charges only			31.76	890	−77.7	0.0	0.0	0.0

[a]With Hamiltonian from Eqs. (25), (26), (28) or (30).
[b]Solute's electronic contribution, Eq. (31).
[c]From Eq. (32).
[d]Including induced reaction field.

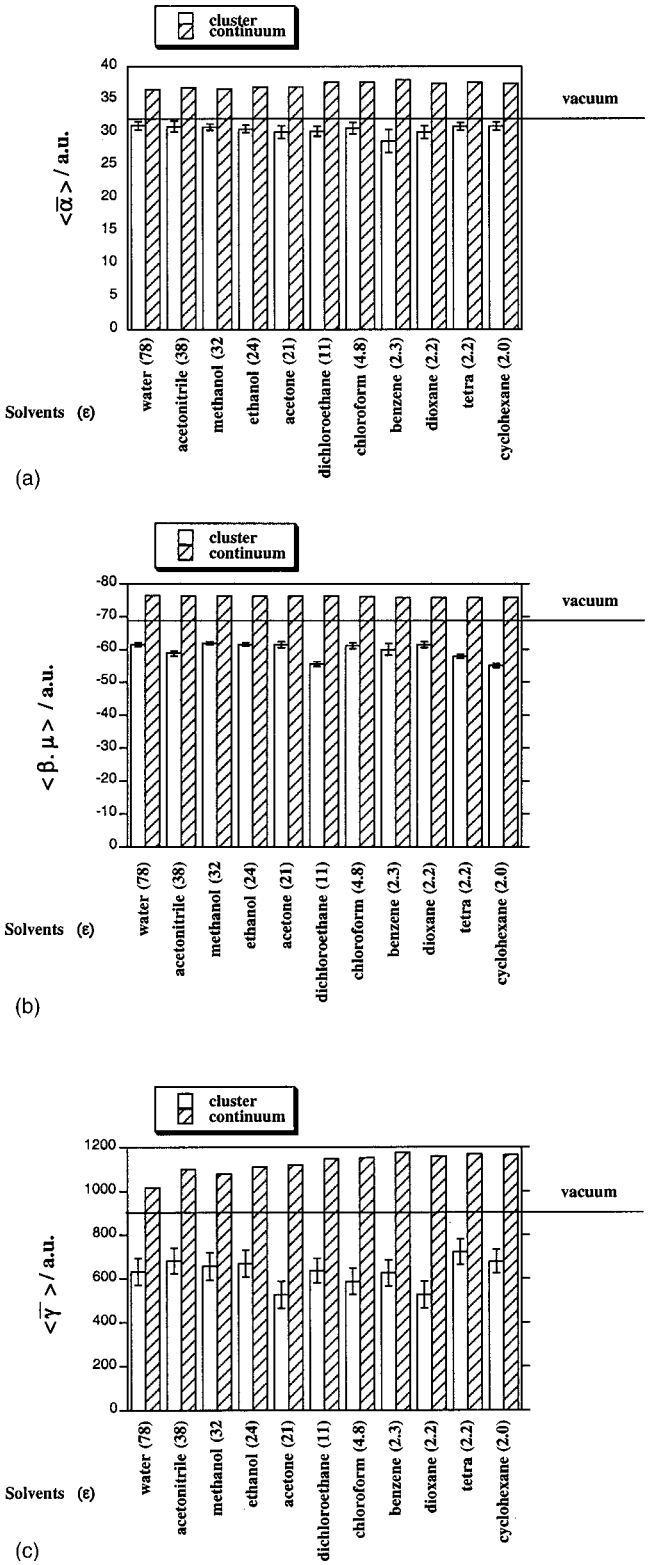

FIG. 3. (a)–(c) CPHF/DRF results for acetone in several solvents with the DZV basis.

B. (Hyper)polarizabilities of acetone in various solvents

Here we report mean linear and hyperpolarizabilities of acetone in eleven solvents spanning a wide range of dielectric properties (see Table IV for details). The solvents were—in separate calculations—modeled both as a dielectric continuum and as clusters of (40 to 50) discrete classical molecules. For the continuum model the Poisson's equations were solved with the boundary element method (BEM) (Ref. 42) using the (modified) programs GEPOL83 (Refs. 49–52) (adapted to HONDO) to construct the boundary between the solute and the solvent. To define the distance between the boundary and the atoms, the radii of the initial spheres in GEPOL around the atoms were taken as the sum of the atomic radius at hand and the formal solvent radius (see Table IV).

In the cluster approximation we first performed classical MD simulations at 298 K using DRF90 (Ref. 31) with its polarizable force field for each of the solute/solvent combinations with rigid solute and solvent molecules. The clusters were constrained to a sphere with a radius chosen such that the density was approximately that of the experimental solvent density. For technical reasons we kept the solute fixed in space. After equilibration we selected randomly a hundred solute/solvent configurations from a 50 ps production run which were subsequently used in the QM/MM calculations described in the previous section, using a DZV basis[47] set in HONDO/DRF. Here we expanded the inducing and response potentials and fields around the solute's atomic centers.[24]

All model formal atomic charges were taken as dipole preserving charges[53] from vacuum *ab initio* HF-SCF calculations using a DZP basis set[47] on the monomers, while all atomic radii (when needed) were taken as Frecer's charge dependent radii.[54] Polarizabilities were taken from Ref. 40. In the MD simulations we applied the atomic polarizabilities for the solute. In all calculations the molecular (group) polarizabilities were used for the solvent molecules as obtained from Ref. 40. An application with the atomic representation of the solvent polarizability gave no significantly different results. Although the dispersion is included in the MD simulations, this is neglected in the QM/MM calculations because the effect on these one-electron properties is expected to be small.[29]

VI. RESULTS AND DISCUSSION

First, we present in Table V the results of a single solute/solvent configuration for acetone in acetone in order to discuss the effects of various options and basis sets.

Typical values during a run for $\bar{\alpha}^{\mathrm{CPHF}}$ as they come from our CPHF Hamiltonian [Eq. (25) or (26)]—which contain the polarization of the classical parts—are also collected in here, together with the uncorrected ($\bar{\alpha}^{\mathrm{raw}}$) and corrected [Eq. 23(a)] solute's electronic contribution ($\bar{\alpha}^{\mathrm{corr}}$). We note that the qualitative behavior is the same for all three basis sets, i.e., $\bar{\alpha}$, $\bar{\gamma}$, and $|\boldsymbol{\beta}\cdot\boldsymbol{\mu}|$ become smaller in the cluster calculations. The bulk correction reinforces this effect. In contrast, the continuum results (so far only obtained for the smaller basis sets) change in the opposite direction. We conclude that the DZP and DZV basis sets behave similarly, and since the former takes an order more of CPU time, we decided to use the latter in the QM/MM calculations for the more than thousand solute/solvent configurations defined above. The last row of Table V shows that the changes in (hyper)polarizabilities are due to the solute's polarizable environment. It is satisfying that the large Sadlej basis gives qualitatively the

TABLE VI. Results (atomic units) of QM/MM calculations for various solvents. Averages are over 100 configurations for each solvent.

Solvent model	Cluster				Continuum			
property	$\langle\lvert\mu\rvert\rangle$	$\langle\overline{\alpha}\rangle$	$\langle\overline{\gamma}\rangle$	$\langle\boldsymbol{\beta}\cdot\boldsymbol{\mu}\rangle$	$\lvert\mu\rvert$	$\overline{\alpha}$	$\overline{\gamma}$	$\boldsymbol{\beta}\cdot\boldsymbol{\mu}$
vacuum	1.46	31.99	898	−68.4				
dzp	1.32	33.35	802	−56.6				
solvent (ε)								
water (78)	1.76±0.10	30.99±0.62	632±87	−61.5±4.6	1.55	36.56	1015	−76.3
acetonitrile (38)	1.65±0.09	30.85±0.79	682±88	−58.9±7.3	1.51	36.73	1098	−76.2
methanol (32)	1.73±0.11	30.76±0.50	656±77	−61.9±5.7	1.52	36.57	1079	−76.2
ethanol (24)	1.65±0.10	30.49±0.56	670±98	−61.6±7.5	1.51	36.89	1109	−76.2
acetone (21)	1.72±0.09	30.06±0.91	527±116	−61.4±6.4	1.50	36.88	1120	−76.2
dzp	1.58±0.09	31.39±0.88	442±119	51.6±5.6	1.38	38.44	998	−62.9
dichloroethane (11)	1.63±0.06	30.17±0.76	637±72	−55.6±6.2	1.50	37.57	1145	−76.2
chloroform (4.8)	1.61±0.04	30.56±0.87	588±89	−61.1±7.4	1.49	37.58	1152	−76.1
benzene (2.3)	1.59±0.07	28.74±1.72	627±168	−60.0±11.5	1.48	37.98	1176	−75.8
dioxane (2.2)	1.72±0.09	30.06±0.91	527±116	−61.4±6.4	1.47	37.42	1159	−75.7
tetra (2.2)	1.48±0.01	30.89±0.58	723±75	−57.9±6.5	1.47	37.59	1167	−75.8
cyclohexane (2.0)	1.49±0.01	30.90±0.58	679±84	−55.1±6.6	1.47	37.45	1164	−75.9

same results, but in what follows we have to keep in mind that the smaller basis sets exaggerate the solvent effects.

Application of the Lorentz factor requires—just like in other cases—first of all a''solvated'' wave function, which means that one has also the ''proper'' field factors. Since the Lorentz factor for acetone is about the same as the factor for the continuum case we do not expect much effect there. But we went through the exercise for the discrete case in the DZV basis—although using other (''improper'') field factors is putting the cart before the horse. The ''Lorentz'' numbers in Table V show an increase of about 8% in $\overline{\alpha}$, and about 60% in $|\boldsymbol{\beta}\cdot\boldsymbol{\mu}|$ and $\overline{\gamma}$, relative to the ''bulk'' numbers. Insofar as these percentages are correct, the use of Lorentz factors lead indeed to serious errors.[2]

In Fig. 3 and Table VI we report values of $\langle\overline{\alpha}\rangle$, $\langle\overline{\gamma}\rangle$, and $|\boldsymbol{\beta}\cdot\boldsymbol{\mu}|$, i.e., the averages over the various solute/solvent configurations from the discrete approach and from the continuum model.

The continuum results are qualitatively the same as those coming from similar treatments,[8,11,55,56] i.e., all properties computed are numerically larger than their respective vacuum values. Local fields are only considered and applied in the work of Macac *et al.*[56] but they use an expansion for the induced dipole [their Eqs. (8) and (9)] which differs from our Eq. (21).

Poulsen *et al.*[57,58] developed a method which is very much like our (exact) DRF approach, i.e., the solvent is modeled either by a continuum or with discrete classical molecules carrying charges and polarizabilities. They find an increase in the (non)linear properties in the continuum model and—a smaller—increase in the discrete approach. However, they use only mean polarizabilities on the solvent molecules and the ''liquid'' is represented by a single (''averaged'') configuration. Local fields are mentioned but not considered further.

In striking contrast, all (averaged) values from our discrete approach are smaller than in vacuum. The error margins for the cluster results are the rms deviations over the configurations analyzed. Since we kept the solute fixed in space the first hyperpolarizability does not vanish on averaging as it should in a real solution, but $|\boldsymbol{\beta}\cdot\boldsymbol{\mu}|$ goes more or less to its vacuum value. In particular with acetonitrile, dichloroethane, tetrachloromethane, and cyclohexane as solvents the average is significantly (i.e., with respect to the rms deviations) smaller than the vacuum value, probably indicating insufficient sampling and/or persisting solvent structure around the solute. We note that all changes (continuum or discrete) w.r.t vacuum are not strongly dependent on the solvent dielectric constants, which is in contrast to the results of Cammi,[8] Luo,[10] and Dehu.[11] For the continuum approach we need a fairly large ''gap'' between the boundary and the atoms because we do not use a single center, but a distributed multipole expansion[24] for (reaction) potentials and fields, the poles of which are closer to the boundary than the solute's center of gravity. Hence, the effect of the perturbation by the ''solvent'' on the wave function is modest. Next, the external field is considered to be optical and has approximately the same effect in all solvents since the refractive indices are approximately the same. The variations in the cluster results are at first sight larger than in the continuum results, but if one accounts for the various rms errors no significant solvent dependency emerges. This comes most likely from the competition between molecular size and shape on the one hand, and the polarizability (or dielectric constant) on the other hand of the various solvents. The formal radius defines the solute/boundary distance in the continuum model, while in the cluster model they regulate the average distance between solute and solvent molecules and the average number of the latter in the first shells. The change in dipole in Table VI gives an indication about how the zeroth order wave function changes on solvation and, for the reasons given above, it is fairly constant as are the perturbations in the external field.

Finally, we note that for ''acetone in acetone'' the polarizability obtained from the experimental refractive index is indeed smaller than in the gas phase (see Table IV). The difference is much smaller than calculated in the present work, but at least it is consistent.

VII. SUMMARY AND CONCLUSIONS

We have developed a consistent scheme for computing (hyper)polarizabilities for quantum chemically treated systems embedded in a classical environment modeling some condensed phase in the frame work of our DRF method taking into account the effect of local fields. The method—with its discrete solvent molecules—is generous to important microscopic details like the instantaneous anisotropies in the solute–solvent interactions. Macroscopically homogeneous solutions were simulated by generating many solute–solvent configurations which were subject to QM/MM calculations to obtain properties over which was averaged. The results are more or less drastically different from approaches in which first the solvent is assumed to be homogeneous (continuum methods) or where first an ''average configuration'' is defined. Because of the sheer number of QM/MM calculations necessary in this approach we had to use a basis set that is (too) small for in particular the second hyperpolarizability. Hence our results are only qualitative, but they lead for acetone in eleven very different solvents systematically to (hyper)polarizabilities which are smaller than the gas phase values if the first few solvent shells are treated explicitly, in contrast to continuum solvent models. We present some evidence that the usual Lorentz field factor, more or less usual in extracting hyperpolarizabilities from experimental susceptibilities, may introduce errors of 50% or more.

We solved the local fields problem within the approximation that the response of the classical parts is strictly linear. We consider this not a serious restriction since higher order interactions tend to be rather small, in particular in liquids. Because of this assumed linear response, all local field factors can be obtained from a set of linear equations by applying a unit external field prior to any quantum chemical calculation. In fact, (model) local field factors could be calculated for correcting experimental results as long as reasonable information about structures is available.

For this paper we used only the coupled perturbative Hartree–Fock method, but the local field corrections are generally applicable, i.e., also for wave functions for which CPHF cannot be used or in finite field calculations.

We will in the near future develop a method to treat frequency dependent polarizabilities along the same lines.

ACKNOWLEDGMENT

The authors are grateful to Dr. Frecer for allowing the use of his data prior to publication.

[1] D. M. Bishop, Int. J. Radiat. Phys. Chem. **13**, 21 (1994).
[2] R. Wortmann and D. M. Bishop, J. Chem. Phys. **108**, 1001 (1998).
[3] B. F. Levine and C. G. Bethea, J. Chem. Phys. **63**, 2666 (1975).
[4] C. C. Teng and A. F. Garito, Phys. Rev. B **28**, 6766 (1983).
[5] M. Stähelin, D. M. Burland, and J. E. Rice, Chem. Phys. Lett. **191**, 245 (1992).
[6] M. Stähelin, C. R. Moylan, D. M. Burland, A. Willets, J. E. Rice, D. P. Sheldon, and E. A. Donley, J. Chem. Phys. **98**, 5595 (1993).
[7] C. J. F. Böttcher and P. Bordewijk, *Theory of Electric Polarization* (Elsevier, Amsterdam, 1978).
[8] R. Cammi, M. Cossi, and J. Tomasi, J. Chem. Phys. **104**, 4611 (1996).
[9] R. Cammi, M. Cossi, B. Mennucci, and J. Tomasi, J. Chem. Phys. **105**, 10556 (1996).
[10] Y. Luo, P. Norman, and H. Ågren, J. Chem. Phys. **109**, 3589 (1998).
[11] C. Dehu, V. Geskin, A. Persoons, and J.-L. Brédas, Eur. J. Org. Chem. **1998**, 1267.
[12] P. Th. van Duijnen, M. Swart, and F. Grozema, in *ACS Symposium Series*, edited by J. Gao and M. A. Thompson (ACS, Washington, D.C., 1998), Vol. 712, p. 220.
[13] J. Tomasi and M. Persico, Chem. Rev. **94**, 2027 (1994).
[14] A. Morita and S. Kato, J. Chem. Phys. **110**, 11987 (1999).
[15] A. H. de Vries, P. Th. van Duijnen, and A. H. Juffer, Int. J. Quantum Chem., Quantum Chem. Symp. **27**, 451 (1993).
[16] P. Th. van Duijnen and A. H. de Vries, Int. J. Quantum Chem., Quantum Chem. Symp. **29**, 523 (1995).
[17] S. Miertus, E. Scrocco, and J. Tomasi, Chem. Phys. **55**, 117 (1981).
[18] D. M. Chipman, J. Chem. Phys. **104**, 3276 (1996).
[19] D. M. Chipman, J. Chem. Phys. **106**, 10194 (1997).
[20] C-G. Zhan and D. M. Chipman, J. Chem. Phys. **109**, 10543 (1998).
[21] D. M. Chipman, J. Chem. Phys. **110**, 8012 (1999).
[22] D. M. Chipman, J. Chem. Phys. **112**, 5558 (2000).
[23] B. T. Thole and P. Th. van Duijnen, Theor. Chim. Acta **55**, 307 (1980).
[24] A. H. de Vries, P. Th. van Duijnen, A. H. Juffer, J. A. C. Rullmann, J. P. Dijkman, H. Merenga, and B. T. Thole, J. Comput. Chem. **16**, 37 (1995).
[25] M. Dupuis, A. Farazdel, S. P. Karma, and S. A. Maluendes, in *MOTECC-90*, edited by E. Clementi (ESCOM, Leiden, 1990), Vol. 277.
[26] M. F. Guest, J. H. van Lenthe, J. Kendrick, and P. Sherwood, GAMESS(UK) (6.2) (Daresbury Laboratory, Cheshire, England, 1999).
[27] M. C. Zerner, ZINDO, A General Semiempirical Program Package (Quantum Theory Project, University of Florida, Gainesville, FL).
[28] A. H. de Vries and P. Th. van Duijnen, Int. J. Quantum Chem. **57**, 1067 (1996).
[29] F. Grozema and P. Th. van Duijnen, J. Phys. Chem. A **102**, 7984 (1998).
[30] P. T. van Duijnen, F. Grozema, and M. Swart, J. Mol. Struct.: THEOCHEM **464**, 191 (1999).
[31] M. Swart and P. Th. van Duijnen, J. Comput. Chem. (submitted).
[32] F. Grozema, R. W. J. Zijlstra, and P. Th. van Duijnen, Chem. Phys. **246**, 217 (1999).
[33] J. Applequist, J. R. Carl, and J. K. Fung, J. Am. Chem. Soc. **94**, 2952 (1972).
[34] J. Applequist, Acc. Chem. Res. **10**, 79 (1977).
[35] B. T. Thole, Chem. Phys. **59**, 341 (1981).
[36] J. A. C. Rullmann and P. Th. van Duijnen, Mol. Phys. **63**, 451 (1988).
[37] L. Jensen, P. Th. van Duijnen, and J. G. Snijders, J. Chem. Phys. (in press).
[38] J. D. Augspurger and C. E. Dykstra, Int. J. Quantum Chem. **43**, 135 (1992).
[39] B. Kirtman, C. E. Dykstra, and B. Champagne, Chem. Phys. Lett. **305**, 132 (1999).
[40] P. Th. van Duijnen and M. Swart, J. Phys. Chem. A **102**, 2399 (1997).
[41] A. H. Juffer, E. F. F. Botta, B. A. M. van Keulen, A. van der Ploeg, and H. J. C. Berendsen, J. Comput. Phys. **97**, 144 (1991).
[42] P. Th. van Duijnen, A. H. Juffer, and J. P. Dijkman, J. Mol. Struct.: THEOCHEM **260**, 195 (1992).
[43] P. Th. van Duijnen and A. H. de Vries, Int. J. Quantum Chem. **60**, 1111 (1996).
[44] F. Sim, S. Chin, M. Dupuis, and J. E. Rice, J. Phys. Chem. **97**, 158 (1993).
[45] S. F. Boys and F. Bernardi, Mol. Phys. **19**, 553 (1970).
[46] A. J. Sadlej, Theor. Chim. Acta **81**, 339 (1992).
[47] T. H. Dunning and P. J. Hay, in *Methods in Electronic Structure Theory*, edited by H. F. Schaefer III (Plenum, New York, 1977), Vol. 1.
[48] P. Th. van Duijnen, M. Dupuis, and B. T. Thole, 1986, IBM DSD, KGN-38.
[49] J. L. Pascual-Ahuir, E. Silla, J. Tomasi, and R. Boncorsi, J. Comput. Chem. **8**, 778 (1987).
[50] J. L. Pascual-Ahuir and E. Silla, J. Comput. Chem. **11**, 1047 (1990).
[51] J. L. Pascual-Ahuir, E. Silla, and I. Tunon, J. Comput. Chem. **15**, 1127 (1994).
[52] E. Silla, I. Tunon, and J. L. Pascual-Ahuir, J. Comput. Chem. **12**, 1077 (1991).
[53] B. T. Thole and P. Th. van Duijnen, Theor. Chim. Acta **63**, 209 (1983).
[54] V. Frecer (personal communication, Trieste, 2000).

[55] T. R. Cundari, H. A. Kurtz, and T. Zhou, J. Phys. Chem. A **104**, 4711 (2000).
[56] P. Macac, P. Norman, Y. Luo, and H. Ågren, J. Chem. Phys. **112**, 1868 (2000).
[57] T. D. Poulsen, P. R. Ogilby, and K. V. Mikkelsen, J. Chem. Phys. **115**, 7843 (2001).
[58] T. D. Poulsen, P. R. Ogilby, and K. V. Mikkelsen, J. Chem. Phys. **116**, 3730 (2002).